Biomedical Research and Therapy, 6(3):3040- 3052

Original Research

Determination of electrophysiological properties of human monocytes and THP-1 cells by dielectrophoresis

Rafeezul Mohamed[1,*], Mohd Azhar Abdul Razak[2], Nahrizul Adib Kadri[3]

ABSTRACT

Introduction: Dielectrophoresis (DEP) is based on polarization and bioparticle movement in applied electric fields. Each type of cells has its own electrical properties within the DEP spectra and undergoes significant changes in direction of frequency following an increase of an applied non-uniform alternating current (AC) electric field. Therefore, DEP can be an effective technique for characterization and separation of different cells. The goal of the current study was to determine the electrophysiological properties of human monocytes and a human monocytic cell line originated from an acute monocytic leukemia patient (THP-1), using a lab on a chip (LOC) device that utilised microarray dot electrodes. **Methods**: Ten microliters of human monocytes isolated from peripheral blood mononuclear cells and highly confluent THP-1 cells were diluted in DEP medium and added to the spacer of the LOC device. Subsequently, the AC signal in the range of 10 kHz to 2 MHz was supplied to the LOC device, and the dynamic behaviours of monocytes and THP-1 cells due to the DEP force were observed. Images were captured and analyzed using MATLAB software. **Results**: Microscopic visualization showed that THP-1 cells were physically larger than human monocytes. The dielectric parameters (radius, diameter, and conductivity and permittivity of the cytoplasm and membrane) were greater for THP-1 cells compared to monocytes. The cross-over frequencies for THP-1 cells and monocytes were respectively 66 kHz and 280 kHz. **Conclusion**: In conclusion, the DEP spectra reflected the morphological differences between monocytes and THP-1 cells. The dielectric properties for each type of cells can be used as the criteria in the development of DEP-based characterization assays.

Key words: Dielectrophoresis, Lab on a Chip, Monocytes, THP-1 cells

[1]*Regenerative Medicine Cluster, Advanced Medical and Dental Institute, Universiti Sains Malaysia*

[2]*Faculty of Electrical Engineering, Universiti Teknologi Malaysia*

[3]*Department of Biomedical Engineering, Faculty of Engineering, University of Malaya*

Correspondence

Rafeezul Mohamed, Regenerative Medicine Cluster, Advanced Medical and Dental Institute, Universiti Sains Malaysia

Email: rafeezul@usm.my

History

- Received: Oct 16, 2018
- Accepted: Mar 14, 2019
- Published: Mar 31, 2019

DOI :

https://doi.org/10.15419/bmrat.v6i3.527

INTRODUCTION

The efficiency of separation and purification techniques is important in studies of leukocyte subpopulations[1]. Existing cell sorting approaches, such as fluorescence activated cell sorting (FACS)[2], magnetic cell sorting[3], and pillar-based microchips[4] have become methods of choice for isolating leukocyte subpopulations. All these sorting approaches are based on the markers expressed on the cell surface[5]. However, these methods involve several preparations and require expensive and bulky equipment such as large magnets, flow cytometers, columns, and centrifuges[1]. Therefore, a new economical sorting device with the ability to discriminate cells, which is compliant with automated and microfluidic applications, is needed[1]. Dielectrophoresis (DEP) stimulates particle movement following interaction with a non-uniform alternating current (AC) electric field[6]. The positive DEP (p-DEP) response occurs when the particles move towards the electrode edge, where a high electric field gradient is present[7]. When the particles move away from the electrode edge, the response is known as negative DEP (n-DEP)[7]. During DEP, particles respond uniquely to different frequencies as they consist of different electrical potentials[8].

DEP effects develop from a non-uniform electric field generated by an electrode. In early DEP studies, electrodes were fabricated from plates, thin metal wires, and needles[9,10]. However, today's advanced micro fabrication technologies facilitate fabrication of DEP platforms based on microelectrode arrays that are able to generate strong DEP forces even when small voltages are applied[11,12]. The best-known electrode structures are planar and three-dimensional[13]. In the current study, standard photolithographic processes were used to fabricate a 4 × 4 microarray dot electrode. Yafouz *et al.*[14] described the fabrication process in detail. Similar electrode geometry was used in a previous study designed to characterize cells in homogenous populations[15]. Dot electrode geometry offers several advantages, such as confined and well-defined analysis areas, efficient electric range infiltration, and an axis symmetry that allows electrical territory dissemination[15].

Numerous researchers are working on developing a non-invasive separation device to characterize cells

Cite this article : Mohamed R, Abdul Razak M A, Kadri N A. **Determination of electrophysiological properties of human monocytes and THP-1 cells by dielectrophoresis**. *Biomed. Res. Ther.;* 6(3):3040-3052.

based on dielectric parameters[16]. DEP has been widely used in cell lysis research[17] and in characterisation of a variety of yeasts[18] and human cells, such as nerve cells[19], platelets[20], sperm cells[21], cancer cells[22], and leukaemia cells[23]. Many studies have been conducted to determine the dielectric properties of human whole blood[24], T and B lymphocytes[25,26], and erythrocytes[27].

With the ultimate quest to develop a Lab on a Chip (LOC) device-based sorter that uses a microarray dot electrode, this study was conducted to firstly characterize the dielectric properties (radius, diameter, and conductivity and permittivity of the cytoplasm and membrane) of human monocytes and a human monocytic cell line originated from an acute monocytic leukemia patient (THP-1). In addition, the cross-over frequency of each cell type was also determined.

METHODS

Cells, cell culture medium, and reagents

THP-1 cells were purchased from the American Type Culture Collection (ATCC, Manassas, VA, USA). Roswell Park Memorial Institute (RPMI)-1640, fetal bovine serum (FBS), penicillin and streptomycin, and phosphate-buffered saline (PBS) were obtained from Thermo Fisher Scientific (Waltham, MA, USA). Anti-human CD3 FITC, anti-human CD14 FITC and anti-human CD14 PE were obtained from BD Biosciences (San Jose, CA, USA).

Culturing human monocytes and THP-1 cells

To isolate monocytes, 40 mL of freshly collected human blood from healthy volunteers (Universiti Sains Malaysia human ethical approval: USM/JEPeM/140384) were diluted in two volumes of PBS supplemented with 2 mM ethylenediaminetetraacetic acid (EDTA) (Thermo Fisher Scientific, Waltham, MA, USA). The diluted cell suspension was carefully layered onto 15 mL of Ficoll Histopaque (GE Healthcare Life Sciences, Malborough, USA), and then centrifuged at 300 g for 40 min at room temperature in a swinging bucket rotor (brakes off). Following centrifugation, the top layer was pipetted off without disturbing the mononuclear cell layer at the interface. The interface of cells was carefully transferred using a Pasteur pipette into a fresh 50 mL conical tube followed by centrifugation at 300 g for 5 min at 4°C. Trace amounts of erythrocytes in the cell suspensions were removed using a human erythrocyte lysing kit (R&D Systems, Minnesota, USA) according the manufacturer's protocols. The cell suspension was centrifuged at 300 g for 5 min, and then, cells were lysed in 5 mL of erythrocyte lysis buffer for 5 min at room temperature. Following incubation, the cell suspension was washed with PBS and centrifuged for 5 min at 300 g. The supernatant was discarded and the cell pellet, which consisted of peripheral blood mononuclear cells (PBMCs), was resuspended in PBS. A haemocytometer was used to count the cells under a light microscope. Phenotypic expression of CD3 and CD14 were determined by BD FACS CANTO II (BD Bioscience, San Jose, CA, USA).

Subsequently, 10 x 10^6 PBMCs were seeded in a T25 cell culture flask and left to adhere in a 5% CO_2 incubator for 2h in complete RPMI medium. Non-adherent cells were discarded and the remainder were washed twice with 3 mL of sterile PBS to completely remove non-adherent cells. Subsequently, 2 mL of complete RPMI were added to the flask, and adherent cells were carefully scrapped off the sides of the flask using a cell scraper. The removed adherent cells were placed in a new 50 mL tube. The flask was then observed under an inverted microscope to identify any remaining cells. If cells were present, complete RPMI medium was added and the scrapping process was repeated. The tube containing the adherent cells was centrifuged at 300 g for 5 min at room temperature. The supernatant was then pipetted off and 1 mL of complete RPMI medium was added to resuspend the cell pellet containing monocytes. Phenotypic expression of CD3 and CD14 were determined by BD FACS CANTO II (BD Bioscience, San Jose, CA, USA).

THP-1 cells were cultured in complete RPMI 1640 supplemented with 10% FBS and 1% penicillin/streptomycin. After the cells reached 90% confluency, they were transferred into a 15 mL centrifuge tube and centrifuged at 300 g for 5 min. After the supernatant was discarded, 1 mL of complete RPMI medium was added to resuspend the cell pellet. A haemocytometer was used to count the cells under a light microscope. Phenotypic expression of CD14 were determined by BD FACS CANTO II (BD Bioscience, San Jose, CA, USA).

After monocytes and THP-1 cells were counted, the cells were centrifuged at 300 g for 5 min in separate tubes. Next, 2 mL of DEP medium (280 mM D-mannitol solution (Sigma Aldrich, Missouri, USA)) were added to each tube after discarding the supernatant. The mixtures were centrifuged again at 300 g for 5 min. The supernatant was discarded, and 1 mL of DEP medium was added to each tube. Finally, 1 x 10^6 monocytes and THP-1 cells were used to determine their electrical properties using a LOC device.

DEP theory, DEP device and operation

Yafouz *et al.*[28] described in detail DEP theory, DEP device and operation procedures. The DEP force (F_{DEP}) applied on a spherical particle of radius r is represented by the equation:

$$\left\langle \overrightarrow{F}_{DEP} \right\rangle = 2\pi r^3 \varepsilon_0 \varepsilon_m Re\left[K(\omega)\right] \nabla E^2 \quad (1)$$

ε_0 and $\varepsilon_m$are respectively defined as the permittivity values of the free space and the relative permittivity of the surrounding medium; ∇E is the electric field gradient; and Re[K(ω)] is an important part of the Clausius-Mossotti factor. The Clausius-Mossotti factor is represented by:

$$K(\omega) = \frac{\varepsilon_p^* - \varepsilon_m^*}{\varepsilon_p^* + 2\varepsilon_m^*} \quad (2)$$

ε_p* and ε_m* are defined as complex permittivity of the particle and the medium respectively, whereby the complex permittivity is stated as:

$$\varepsilon^* = \varepsilon - \frac{j\sigma}{\omega} \quad (3)$$

ε is the permittivity, ω is the angular frequency, j is the square root of -1 and σ is the material conductivity. The F_{DEP} turns zero at a specific frequency and this phenomenon is known as the crossover frequency (Re[K(ω)] = 0).

The LOC device was a compact of five layers as shown in **Figure 1**. A 4×4 microarray dot electrode was used (**Figure 2**), which was fabricated by our team from Universiti Malaya, led by Associate Professor Dr Nahrizul Adib Kadri. This electrode was fabricated using the standard photolithographic processes. Generally, Gold-coated (24K) with microscopic glass slides from Fisher Scientific, New Hampshire, USA were cut into two pieces to acquire the dimension of 38×26 mm^2. AutoCAD software was used to design microelectrode geometry, and the manufacture of the photomask was performed by JD photo-tools (Oldham, Lancashire, UK). A gold dot microarray electrode was placed on the bottom layer of Indium Tin Oxide (ITO) (15-30 Ω ITO-coated glass slide, SPI Supplies, West Chester, PA, USA), which acted as the ground electrodes counter electrode at the top. The vertical DEP effects generated higher numbers of particles experiencing DEP force.

Experimental set up

5Vp-p sinusoidal electrical signals were supplied to the DEP device by a function generator (Textronix, Beaverton, OR, USA) to provoke the non-uniform electrical range required for DEP. The experiments were carried out by applying one signal to all four dots even though the device was capable of receiving four signals at the same time. For each set of the cells (monocytes and THP-1 cells), 15 individual frequencies in the range of 10 kHz to 2 MHz were transmitted via the microarray dot electrodes. The LOC device was positioned on a microscope stage (BX51, Olympus, Tokyo, Japan), and the plane of the cells was focused to discern the movement of the cells, which was triggered by the DEP force. Images of the cells were captured by a CCD camera (Dino Capture, Torrance, CA, USA), which was placed in one of the microscope eyepieces. The experiment was performed three times for each frequency and each sample. Images were captured after 10 seconds of applying the electrical signal. All images were saved in the dedicated computer for subsequent analysis.

Image analysis

The microscopic images obtained from this experiment were analyzed to evaluate the effects of DEP on monocytes and THP-1 cells to determine their dielectric properties. Initially, the images were segmented into regions of interest (ROIs), in which, the central part of the dot area was segmented into a square shape (**Figure 3**). All images had the same dimensions of 145 × 145 pixels.

The acquired images were converted into binary images with the threshold value of 170 (**Figure 4**). The binary images then were converted into black and white using the built-in function im2bw in MATLAB software (Mathworks, Natick, MA, USA). The function had two parameters, known as 'unsigned integer' and 'level' values. The 'level' values were defined as the values between 0 and 1 that measure the intensity of the level boundary. The value was converted to '0' (black) if it was lower than the boundary level, and to '1' (white) if it was above the boundary level. The total number of black pixels for each image was counted using MATLAB software to measure the light intensity. The alteration of light intensity for each frequency was determined by subtracting the total number of black pixels of an image, without application of the electrical signal applied, from the total number of black pixels of the image with p-DEP and n-DEP effects. The values of light intensity alteration were then normalized and plotted (y-axis) against the applied electrical frequency (x-axis). A single shell dielectric model was used to fit the DEP spectra and identify the radius, membrane specific capacitance, internal conductivity, and permittivity for each cell types.

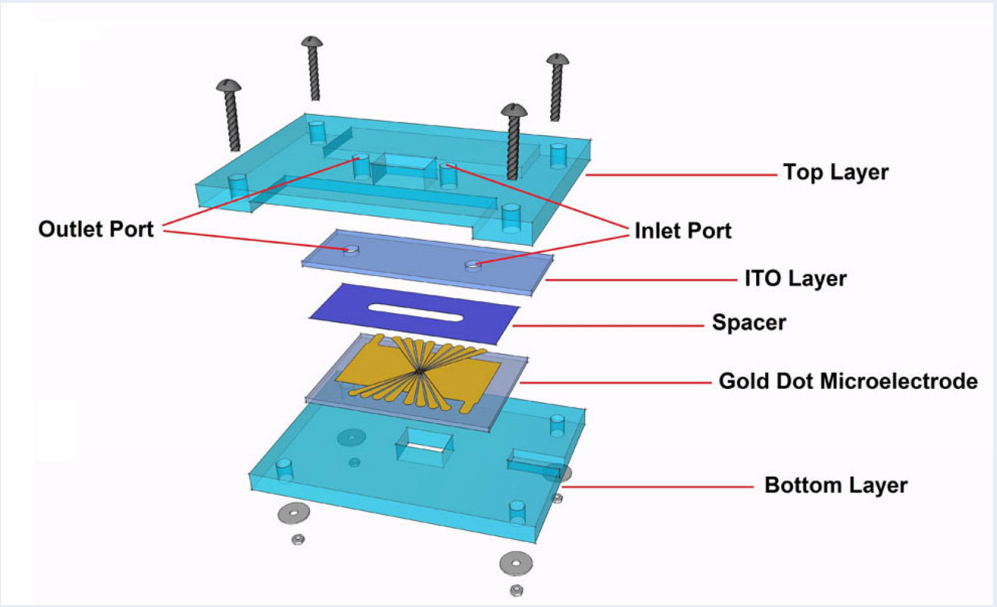

Figure 1: **A Schematic diagram of the LOC device.** It consists of five layers, as the top and bottom device covers were made of 4 mm thick polymethyl methacrylate (PMMA). Indium tin oxide(ITO)-coated glass slides serve as the ground electrodes. The spacer, in whichthe DEP effect occurs, acts as the gasket chamber. The 4 × 4 microarray dotelectrode was fabricated using standard photolithographic processes. A 3 mm channel was designed in the middle of the spacer to create space for the fluid to flow. Flexible wires were soldered to the gold and ITO electrodes via silver-loaded epoxy and were connectedto the function generator which supply electrical signal to the LOC device. The image was reproduced with permission from [13].

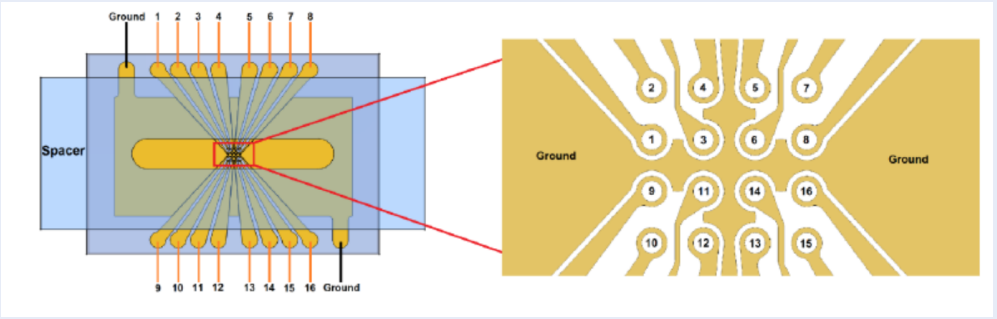

Figure 2: **A 4 × 4 microarray dot electrode**. Sixteen individual inputs can be supplied electrical signal simultaneously.

Statistical analysis

Statistical analysis was conducted using Statistical Package for the Social Sciences (SPSS) version 16.0 (SPSS, Chicago, IL, USA), which assessed the difference in the DEP response between monocyte and THP-1 cells. A t-test was carried out using the individual data points of the intensity shifts at each frequency. A p-value <0.05 was interpreted as statistically significant. The experiment was repeated three times with monocytes isolated from three different donors.

RESULTS

Phenotypic analysis of isolated monocyte and THP-1 cells

Phenotypic analysis of CD3, which represented T lymphocytes, and CD14, representing monocytes, was carried on isolated PBMC and monocytes. Flow cytometry analysis showed that the percentage of $CD3^+$ and $CD14^+$ in PBMC were respectively 54.3%

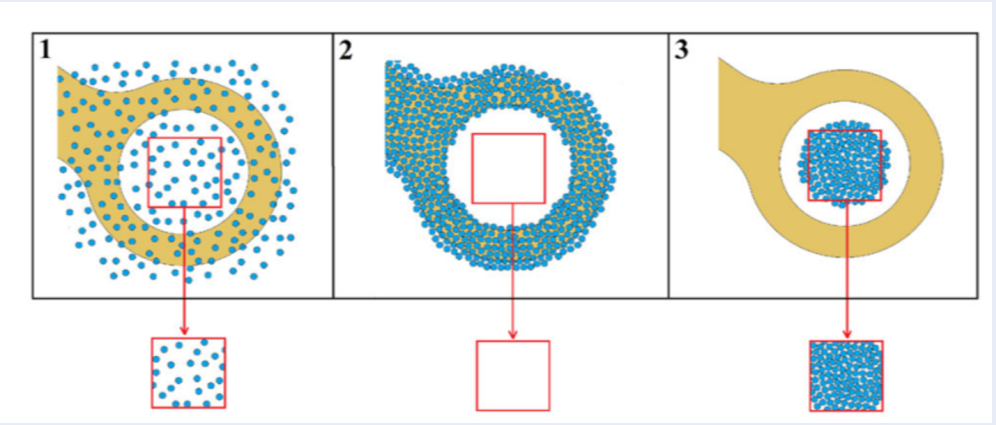

Figure 3: **Segmented region of interest in the square shape for distributed cells** without the application of electrical signal (1), cells with the p-DEP effect (2), andcells with the n-DEP effect (3).

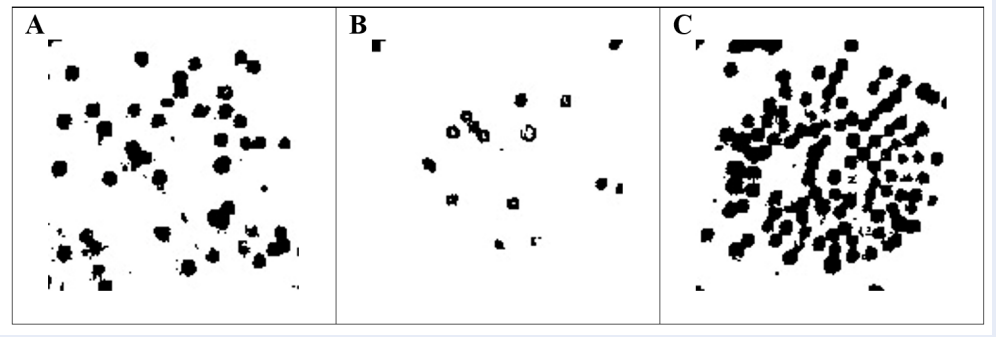

Figure 4: **Segmented binary image with threshold value of 170**. **A**) binary image without the application of electrical signals; **B**) binary image with p-DEP effect (1 MHz); and **C**) binary image with n-DEP effect (10 kHz).

and 0.81% (**Figure 5A**). Following two-hour incubation of PBMC in culture flask and serial washing steps, the percentage of CD3+ and CD14+ in adherent monocyte were 2.18% and 44.5%, respectively (**Figure 5B**). Meanwhile, the percentage of $CD14^{+}$, which represented monocytes in cultured THP-1 cell, was 4.12% (**Figure 5 C**).

Effect of DEP on monocytes and THP-1 cells

Figure 6 shows representative images of DEP effects on monocytes and THP-1 cells on the dot electrode. Monocytes and THP-1 cells were distributed equally within the dot perimeter before the transmission of AC signals (*reference*). When the LOC was supplied with 10 kHz and 1.4 MHz, monocytes and THP-1 cells respectively exhibited n-DEP and p-DEP responses. Image analysis showed that THP-1 cells were physically larger and had weaker p-DEP compared to monocytes.

DEP spectra and dielectric properties

The DEP spectra, which represented the effects of DEP on each cell type, were constructed by plotting the light intensity shift (y-axis) against the electrical frequency applied for the captured images (x-axis). The DEP spectra of monocytes and THP-1 cells were analyzed using a wide range of frequencies to determine their electrophysiological properties based on single shell dielectric model. **Figure 7** shows the DEP spectra for monocytes. The dielectric parameters for the cytoplasm and membrane of monocytes were as follows: cytoplasmic radius = 3.1 μm, conductivity (σ) = 0.011 S/m, permittivity (ε) = 85; and membrane diameter (d) = 0.5 nm, conductivity (σ) = 0.001 uS/m, permittivity (ε) = 0.64.

Figure 8 shows the DEP spectra for THP-1 cells and their electrophysiological properties based on single shell dielectric model. The dielectric properties for THP-1 in the cytoplasm and membrane, which were

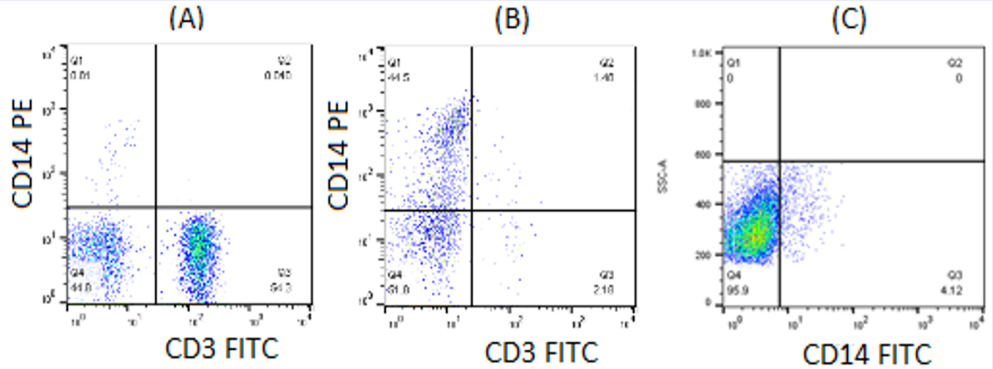

Figure 5: **Phenotypic analysis of isolated PBMC, monocyte andTHP-1 cell.** Isolated PBMC and monocytes were stained with CD3 FITC and CD14 PE. The stained cells were incubated for 30 min in the dark, washed and analysed by flow cytometry. The percentage of CD3+ and $CD14^{+}$ in PBMC were 54.3% and 0.81% respectively (**A**). Meanwhile, the percentage of $CD3^{+}$ and $CD14^{+}$ in adherent monocyte were 2.18% and 44.5% respectively (**B**). On the other hand, the percentage of $CD14^{+}$ which represent monocytes in cultured THP-1 cell was 4.12% (**C**).

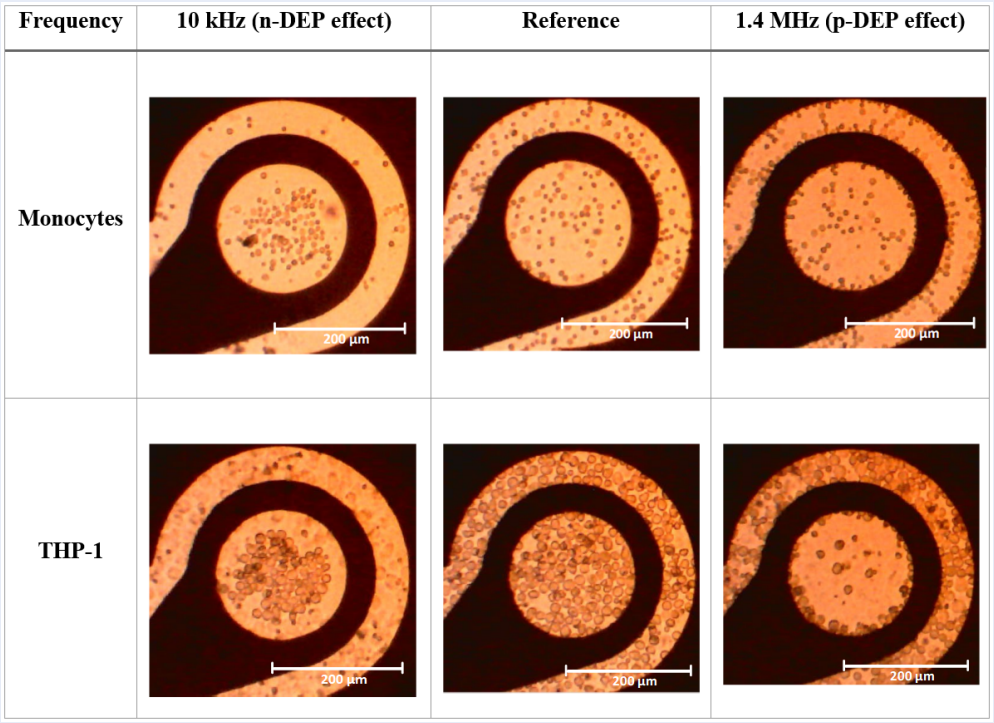

Figure 6: **Representative images of monocytes and THP-1 cells with n-DEP responses, reference state, and p-DEP responses in the dot electrode.** Monocytes and THP-1 cells were distributed equally within the dot perimeter before transmission of the AC signal (reference). Monocyte and THP-1 cells show n-DEP effect after applying the 10 kHz signal (n-DEP effect). However, both cells show p-DEP effect after applying the 1.4 MHz signal.

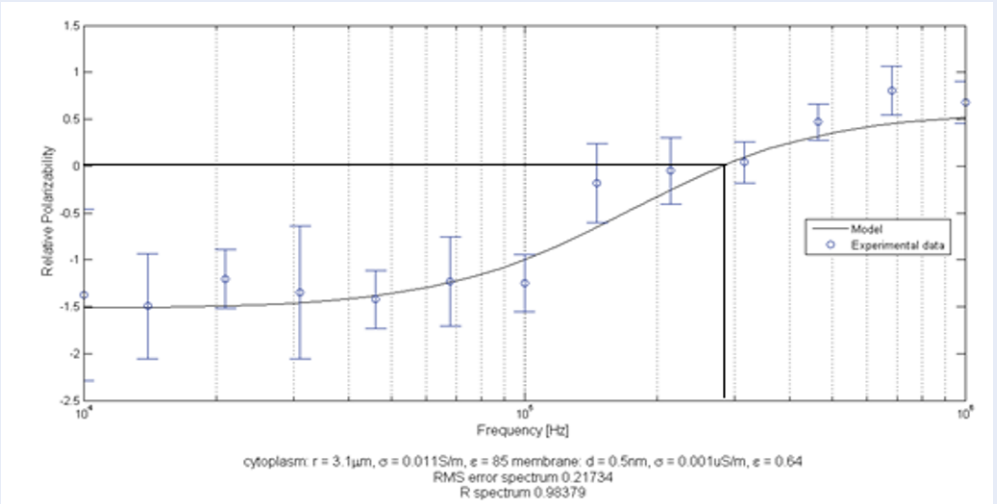

Figure 7: **DEP spectra of monocytes in conductivity medium (0.01 S/m).** The circles (O) on the graph indicate the measured data. Best-fit lines were added to the DEP spectrum of each set of cells using logistic function. The correlation coefficients of the lines were greater than 0.9. The error bars show the standard error of three experiments conducted at each frequency. Continuous curves show best fits of the single-shell dielectric modelfor monocytes. The cross-over frequency for monocytes was 280 kHz.

greater than those of monocytes, were as follows: cytoplasmic radius = 8 µm, conductivity (σ) = 0.109 S/m, permittivity (ε) = 100; and membrane diameter (d) = 8.2 nm, conductivity (σ) = 0.01 uS/m, permittivity (ε) = 3.7.

The cross-over frequencies for monocytes and THP-1 cells were obtained by adding the best fit lines to the DEP spectrum of each cell type. The cell cross-over frequency was defined as the frequency at which there was no occurance of cell movement in response to DEP. At this point, the light intensity was equal to zero. It was shown that the cross-over frequency was 280 kHz for monocytes and 66 kHz for THP-1 cells (**Figures 7 and 8**). Furthermore, statistical analysis showed that there was a significant difference between DEP spectra of monocytes and THP-1 cells ($p<0.05$).

DISCUSSION

Dysfunction of innate immune cells can expose the host to various autoimmune diseases such as rheumatoid arthritis (RA) and systemic lupus erythematosis (SLE). Depletion of PBMCs inhibits RA, while granulocytes can induce RA progression[32]. Alterations of monocyte morphology and function in SLE patients reduce the ability of these cells to perform phagocytosis of bacteria[33]. Thus, the important function of innate immune cells warrant extensive research, and effective techniques for isolating immune cells are critical to the outcome of such studies.

In the current study, a simple and rapid technique for isolating PBMCs and monocytes was used. First, PBMCs were isolated from blood by density gradient centrifugation using Ficoll Histopaque. Following centrifugation, cells and other elements in the blood were separated in the Ficoll Histopaque solution in layers based on their density/size differences[34]. Next, monocytes were isolated from PBMCs using adherence technique. This method has several limitations, such as a high percentage of lymphocyte contamination, low flexibility, high manipulation, and monocyte transient activation[35]. The first hour of monocyte adherence is characterised by high lymphocyte contamination, but it decreases to 40–50% after two washes and is further reduced to 30% after five washes[35]. Bennett *et al.*[36] reported that after four vigorous washes during the first 24h, monocytes were still contaminated with 24% of lymphocytes[36]. Factors such as the number of PBMCs used in the monocyte adherence procedure, the number of washes, vigorous washing, and the duration of adhesion strongly impact the degree of lymphocyte contamination when isolating monocytes using the adherence technique[36]. In the current study, the efficiency of CD3 isolation, which represented T lymphocytes, after 2h of culture and vigorous washing, was about 95.9%. On the other hand, the percentage of CD14 expression increased to about 98% in adherent monocytes.

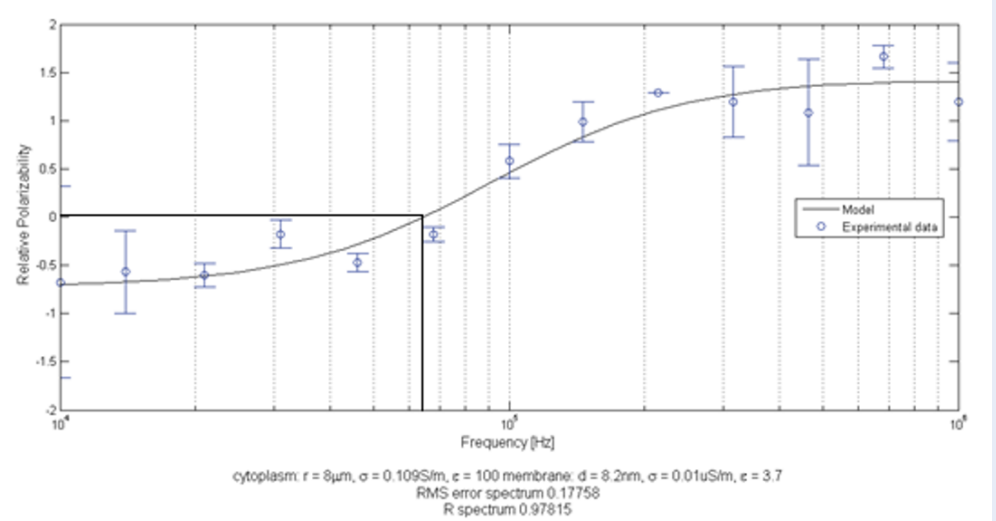

Figure 8: **DEP spectra for THP-1 cells in conductivity medium (0.01 S/m)**. The circles (O) on the graph indicate the measured data. Best-fit lines were added to the DEP spectrum of each set of cells using logistic function. The correlation coefficients of the lines were greater than 0.9. The error bars show the standard error of three experiments conducted at each frequency. Continuous curves show best fits of the single-shell dielectric model for THP-1 cells. The cross-over frequency (the frequency at which the light intensity is equal to zero) for THP-1 cells was 66 kHz.

Table 1: Summary of dielectric parameters for other mammalian cells measured using a microfluidic electrorotation device and analyzed using a single shell dielectric model

Technique	Cell types	Frequency	Dielectric parameters	References
Four electrode in phase quadrature	MDA231, T lymphocytes, and Erythrocytes	1 kHz–1 GHz	MDA231 (26 ± 4.2 mF/m2) T lymphocytes (11 ± 1.1 mF/m2) Erythrocytes (9 ± 0.80 mF/m2)	[29]
Four electrode in phase quadrature	Leukocytes (WBCs)	10 kHz–120 MHz	T-lymphocytes (10.5 ± 3.1 mF/m2) B-lymphocytes (12.6 ± 3.5 mF/m2) Monocytes (15.3 ± 4.3 mF/m2)	[1]
Four electrode in phase quadrature	Leukocytes (WBCs), SkBr3, and A549	10 kHz–10 MHz	T lymphocytes (7.01 ± 0.91 mF/m2) B lymphocytes (10.33 ± 1.6 mF/m2) Granulocytes (9.14 ± 1.06 mF/m2) Monocytes (11.77 ± 2.12 mF/m2) SkBr3 (14.83 ± 1.74 mF/m2)	[30]

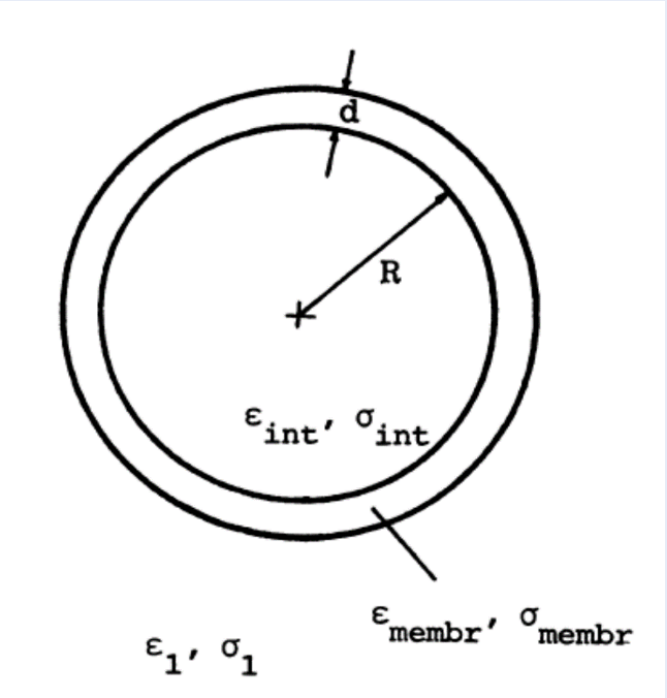

Figure 9: **A single shell dielectric model.** ε is the dielectric permittivity and σ is the electric conductivity. The subscripts, int, membr, and 1, represent cell interior, cell membrane, and suspending medium, respectively. R represent radius of the cell, and d is the membrane thickness. Figure and description were adapted from Marszalek *et al.*[31].

Other techniques for isolating monocytes are available. For example, magnetic activated cell sorting (MACS) technology, which utilises positive selection of classical monocyte-specific markers such as CD14, isolated 90–95% of monocytes ($CD14^+CD16^-$)[37]. Isolation of monocytes by FACS also achieved 95–98% monocyte purity. However, FACS is suitable for isolating intermediate ($CD14^{++}CD16^+$) or non-classical ($CD16^{++}CD14^+$) monocytes, which express different percentages of CD14 and CD16. Both MACS and FACS also have several disadvantages in addition to the requirement of expensive instruments and accessories. Monocytes isolated by MACS technology can be contaminated by the magnetic particles used to label cells[38]. FACS methods reduce the viability of sorted cells due to rapid flow in the machine[38]. THP-1 is a human leukaemia monocytic cell line derived from the peripheral blood of a 1-year old male human with acute monocytic leukemia[39]. THP-1 cells are frequently utilised by researchers to determine monocytic functions[40]. THP-1 cells express low levels of CD14, which is a surface marker for human monocytes, as observed in our flow cytometry data (**Figure 5 C**)[41]. Homogenous genetic background that diminishes donor variability by THP-1 superseded primary monocytes[40]. Furthermore, THP-1 cells are easily accessible and can be purchased directly from ATCC. In contrast, primary human monocytes must be isolated from the peripheral blood of a healthy human donor. Several studies have demonstrated that THP-1 displays a more mature monocytic phenotype compared to those of other immortalized human monocyte cell lines, such as U937 cells[42]. The interaction between THP-1 and endothelial cells also mimics that of human primary monocytes[43–45]. A THP-1 cell is a non-adherent cell and thus can be cultured as a cell suspension.

LOC designs offer an alternative sorting technique, and numerous LOC designs have been invented for various applications. Masuda *et al.*[46] applied DEP in a LOC device to manipulate and discriminate them into different outlets. Fatoyinbo *et al.*[15] fabricated a device composed of a gold 4 × 4 dot-patterned microarray with a parallel ground indium tin oxide microelectrode on top to rapidly measure the dielectric properties of cells. The advantage of the microarray dot electrode approach is that each dot can be energized separately, and cell electrophysiology can be

measured at near real-time speed[13]. A similar LOC device with microarray dot electrodes was used in the current study to measure the DEP effect on monocytes and THP-1 cells.

When monocytes and THP-1 cells were subjected to a non-uniform electric field, two different forces were generated between the cells and the surrounding medium, resulting in DEP effects. The movement of the monocytes and THP-1 cells in response to p-DEP or n-DEP forces occurred due to the relative polarizability of the cells and the DEP medium, which consisted of D-Mannitol to dilute the cells. The 280 mM D-mannitol solution is a low conductivity isotonic solution[47]. Generally, when the high frequency electrical signal was applied, the cells with p-DEP effect became more polarizable than the surrounding medium. When the low frequency electrical signal was applied, the cells with n-DEP effect became less polarizable than the surrounding medium. The images captured during the experiment showed that THP-1 cells had a weaker p-DEP effect than monocytes due to their morphological differences. Microscopic visualisation showed that THP-1 cells were physically larger than monocytes, and the greater size influenced the strength of p-DEP effects.

The light intensity variation between the original images (before the AC signals were transmitted) and the final images (after the AC signal was applied) was calculated to evaluate cell motions in the ROI. The principle of Beer-Lambert's law of light absorption states that the light intensity corresponds to the cell concentration[28]. After AC signals were applied, the light intensity was low for cells with n-DEP effect, as all cells were situated in the middle of the ROI and thus, more black pixels were detected. DEP spectra revealed that the light intensity shifted to the negative side. In contrast, cells with p-DEP effect moved away from the center of the ROI, which increased the light intensity, and fewer black pixels were detected in the image. In this case, the DEP spectra showed that the light intensity shifted to the positive side.

To quantify DEP effects on monocytes and THP-1 cells, DEP spectra of the light intensity shift were plotted against the frequency of the applied AC signals, which ranged from 10 kHz to 2 MHz. The dielectric properties (radius, diameter, and conductivity and permittivity of the cytoplasm and membrane) were determined by adjusting the light intensity shifts towards the shell model that described the cells[48] and conducting the best-fit numerical analysis[49]. This method has been used in many DEP characterization studies[50–53]. In the current study, the dielectric properties of the cytoplasm and membrane of THP-1 cells were greater than those of monocytes. To date, this is the first report of the dielectric properties of THP-1 cells, so no data are available for comparison. The dielectric parameters obtained in this study for monocytes were lower than the values reported by Yang *et al.*[1]. They were comparable to those reported for cytoplasm relative permittivity and conductivity, which were in the range of 50–150 and 0.1–1.3 S/m, respectively[54]. Values of relative permittivity and conductivity of the cell membrane were reported to be approximately 2–15 and 10^{-18}–10^{-4} S/m[54]. Previous estimation of the thickness of the cell membrane were 4–10 nm[55,56]. **Table 1** shows a summary of dielectric parameters for other mammalian cells such as mouse lymphocytes and erythrocytes, human erythrocytes, normal and malignant white blood cells and leukemia cells that were measured using a microfluidic electrorotation device and analyzed using a single shell dielectric model[1,29,30].

Monocytes and THP-1 cells are composed of complex internal and membrane structures. Characterization of electrophysiological properties for both cell types was conducted using a single-shell dielectric model (**Figure 9**), as this model is the most frequently used model for studying cell biology[57–59]. In this model, a cell is assumed to consist of a conductive interior, such as a sphere or an ellipsoid, surrounded by a weak conducting, concentric, and rigid membrane shell[31,60]. AC signal frequencies between 1 kHz and 10 MHz, which are often used in DEP research, mainly produce two cellular dielectric characteristics: plasma membrane capacitance and conductivity[60]. Different cells contain distinct dielectric properties, and therefore, are influenced greatly by any changes in the cell physiology or abnormal cell conditions[1,49,61,62]. Other factors may also influence the dielectric properties of a cell type, such as intracellular and membrane morphology, membrane surface conductance, ion and molecule dispersion, and transport across the membrane[63]. The cell membrane is consisted of lipid, glycolipid, and glycoprotein membrane components, thus, charged molecules may attach to the membrane surface and affect the conductivity and permittivity of the cell membrane[63]. The DEP medium also affects the dielectric properties because each cell may act differently in media with different ionic concentrations[1].

The cross-over frequency is defined as the frequency at which the light intensity is equal to zero. At this point, there is no p-DEP or n-DEP effects on the cells. In this study, the sigmoid shape for both monocytes and THP-1 cells was consistent, and the cross-over frequency respectively occurred at 280 kHz and 66

kHz. These results indicate that monocytes and THP-1 cells have unique cross-over frequencies, which in turn suggests that DEP is a reliable approach for characterising the cells. Huang *et al.*[64] used a silicon-based microchip with interdigitated gold microelectrodes fabricated using standards, a photolithography patterning technique to study characteristics of cells. They found that PBMCs had a wide range of cross-over frequencies, from 35 kHz to 120 kHz, due to the mixed population of cells. They also reported obvious differences in the cross-over frequencies for monocytes (44.6 kHz), natural killer cells (63.2 kHz), B cells (78.8 kHz), and T cells (89.1 kHz).

CONCLUSIONS

In conclusion, the different sizes of monocytes and THP-1 cells may explain the observed differences in dielectric properties between these cell types. The dielectric properties of THP-1 cells, which are often used as a model for primary human monocytes, were greater than those of monocytes. These differences indicate that THP-1 cells may not be the best model for studying human primary monocytes. The dielectric properties for each type of cells can be used as the criteria in the development of DEP-based characterization assays.

ABBREVIATIONS

AC: Alternating current
CD: Cluster of differentiation
CCD: Charge couple device
DEP: Dielectrophoresis
ITO: Indium tin oxide
kHz: kilohertz
LOC: Lab on Chip
MHz: Megahertz
n-DEP: Negative-DEP
PBMC: Peripheral blood mononuclear cell
p-DEP: Positive-DEP

COMPETING INTERESTS

There is no conflict of interest.

AUTHORS' CONTRIBUTIONS

Rafeezul Mohamed carried out the experiment, wrote the manuscript and principal investigator for Universiti Sains Malaysia short term grant.
Mohd Azhar Abdul Razak performed the image analysis.
Nahrizul Adib Kadri fabricated the LOC device.
All the authors read and approved the final manuscript.

ACKNOWLEDGMENTS

This work was supported by a Universiti Sains Malaysia Short Term Grant (304/CIPPT/6313133).

REFERENCES

1. Yang J, Huang Y, Wang X, Wang XB, Becker FF, Gascoyne PR. Dielectric properties of human leukocyte subpopulations determined by electrorotation as a cell separation criterion. Biophys J. 1999;76(6):3307–14. 10354456. Available from: 10.1016/S0006-3495(99)77483-7.
2. Lostumbo A, Mehta D, Setty S, Nunez R. Flow cytometry: a new approach for the molecular profiling of breast cancer. Exp Mol Pathol. 2006;80(1):46–53. 16271361. Available from: 10.1016/j.yexmp.2005.09.007.
3. Kato K, Radbruch A. Isolation and characterization of CD34+ hematopoietic stem cells from human peripheral blood by high-gradient magnetic cell sorting. Cytometry. 1993;14(4):384–92. 7685679. Available from: 10.1002/cyto.990140407.
4. Nagrath S, Sequist LV, Maheswaran S, Bell DW, Irimia D, Ulkus L, et al. Isolation of rare circulating tumour cells in cancer patients by microchip technology. Nature. 2007;450(7173):1235–9. 18097410. Available from: 10.1038/nature06385.
5. Salmanzadeh A, Davalos RV. Isolation of rare cells through their dielectrophoretic signature. J Membr Sci Technol. 2013;3(01):e112. Available from: 10.4172/2155-9589.1000e112.
6. Ramos A, Morgan H, Green NG, Castellanos A. Ac electrokinetics: a review of forces in microelectrode structures. J Phys D Appl Phys. 1998;31(18):2338–53. Available from: 10.1088/0022-3727/31/18/021.
7. Morgan H, Hughes MP, Green NG. Separation of submicron bioparticles by dielectrophoresis. Biophys J. 1999;77(1):516–25. 10388776. Available from: 10.1016/S0006-3495(99)76908-0.
8. Rahman NA, Ibrahim F, Yafouz B. Dielectrophoresis for biomedical sciences applications: A review. Sensors (Basel). 2017;17(3):449. 28245552. Available from: 10.3390/s17030449.
9. Pohl HA, Pethig R. Dielectric measurements using non-uniform electric field (dielectrophoretic) effects. J Phys E Sci Instrum. 1977;10(9):883. Available from: 10.1088/0022-3735/10/9/513.
10. Jones T, Kraybill J. Active feedback-controlled dielectrophoretic levitation. J Appl Phys. 1986;60(4):1247–52. Available from: 10.1063/1.337345.
11. Hamada R, Takayama H, Shonishi Y, Mao L, Nakano M, Suehiro J. A rapid bacteria detection technique utilizing impedance measurement combined with positive and negative dielectrophoresis. Sens Actuators B Chem. 2013;181:439–45. Available from: 10.1016/j.snb.2013.02.030.
12. Martinez-Duarte R, Camacho-Alanis F, Renaud P, Ros A. Dielectrophoresis of lambda-DNA using 3D carbon electrodes. Electrophoresis. 2013;34(7):1113–22. 23348619. Available from: 10.1002/elps.201200447.
13. Yafouz B, Kadri NA, Ibrahim F. Microarray dot electrodes utilizing dielectrophoresis for cell characterization. Sensors (Basel). 2013;13(7):9029–46. 23857266. Available from: 10.3390/s130709029.
14. Yafouz B, Kadri NA, Ibrahim F. The design and simulation of a planar microarray dot electrode for a dielectrophoretic Lab-on-Chip device. Int J Electrochem Sci. 2012;7:12054–63.
15. Fatoyinbo HO, Kadri NA, Gould DH, Hoettges KF, Labeed FH. Real-time cell electrophysiology using a multi-channel dielectrophoretic-dot microelectrode array. Electrophoresis. 2011;32(18):2541–9. 21922496. Available from: 10.1002/elps.201100033.

16. Huang Y, Wang XB, Becker FF, Gascoyne PR. Introducing dielectrophoresis as a new force field for field-flow fractionation. Biophys J. 1997;73(2):1118–29. 9251828. Available from: 10.1016/S0006-3495(97)78144-X.
17. Young CW, Hsieh JL, Ay C. Development of an integrated chip for automatic tracking and positioning manipulation for single cell lysis. Sensors (Basel). 2012;12(3):2400–13. 22736957. Available from: 10.3390/s120302400.
18. Patel S, Showers D, Vedantam P, Tzeng TR, Qian S, Xuan X. Microfluidic separation of live and dead yeast cells using reservoir-based dielectrophoresis. Biomicrofluidics. 2012;6(3):34102. 23853679. Available from: 10.1063/1.4732800.
19. Jaber FT, Labeed FH, Hughes MP. Action potential recording from dielectrophoretically positioned neurons inside microwells of a planar microelectrode array. J Neurosci Methods. 2009;182(2):225–35. 19540265. Available from: 10.1016/j.jneumeth.2009.06.013.
20. Piacentini N, Mernier G, Tornay R, Renaud P. Separation of platelets from other blood cells in continuous-flow by dielectrophoresis field-flow-fractionation. Biomicrofluidics. 2011;5(3):34122–341228. 22662047. Available from: 10.1063/1.3640045.
21. Rosales-Cruzaley E, Cota-Elizondo PA, Sánchez D, Lapizco-Encinas BH. Sperm cells manipulation employing dielectrophoresis. Bioprocess Biosyst Eng. 2013;36(10):1353–62. 23086549. Available from: 10.1007/s00449-012-0838-6.
22. Chuang CH, Huang YW, Wu YT. System-level biochip for impedance sensing and programmable manipulation of bladder cancer cells. Sensors (Basel). 2011;11(11):11021–35. 22346685. Available from: 10.3390/s111111021.
23. Imasato H, Yamakawa T, Eguchi M. Separation of leukemia cells from blood by employing dielectrophoresis. Intelligent Automation and Soft Computing. 2012;18(2):139–52. Available from: 10.1080/10798587.2008.10643232.
24. Schwan HP. Electrical properties of blood and its constituents: alternating current spectroscopy. Blut. 1983;46(4):185–97. 6338980. Available from: 10.1007/BF00320638.
25. Bordi F, Cametti C, Rosi A, Calcabrini A. Frequency domain electrical conductivity measurements of the passive electrical properties of human lymphocytes. Biochim Biophys Acta. 1993;1153(1):77–88. 8241253. Available from: 10.1016/0005-2736(93)90278-8.
26. Beving H, Eriksson LE, Davey CL, Kell DB. Dielectric properties of human blood and erythrocytes at radio frequencies (0.2-10 MHz); dependence on cell volume fraction and medium composition. Eur Biophys J. 1994;23(3):207–15. 7956980. Available from: 10.1007/BF01007612.
27. Ballario C, Bonincontro A, Cametti C, Rosi A, Sportelli L. Effect of extracellular alkali metal salts on the electric parameters of human erythrocytes in normal and pathological conditions (homozygous beta-thalassemia). Z Naturforsch C. 1984;39(11-12):1163–9. 6531948. Available from: 10.1515/znc-1984-11-1230.
28. Yafouz B, Kadri NA, Rothan HA, Yusof R, Ibrahim F. Discriminating dengue-infected hepatic cells (WRL-68) using dielectrophoresis. Electrophoresis. 2016;37(3):511–8. 26530354. Available from: 10.1002/elps.201500282.
29. Becker FF, Wang XB, Huang Y, Pethig R, Vykoukal J, Gascoyne PR. Separation of human breast cancer cells from blood by differential dielectric affinity. Proc Natl Acad Sci USA. 1995;92(3):860–4. 7846067. Available from: 10.1073/pnas.92.3.860.
30. Han SI, Joo YD, Han KH. An electrorotation technique for measuring the dielectric properties of cells with simultaneous use of negative quadrupolar dielectrophoresis and electrorotation. Analyst (Lond). 2013;138(5):1529–37. 23353873. Available from: 10.1039/c3an36261b.
31. Marszalek P, Zielinsky JJ, Fikus M, Tsong TY. Determination of electric parameters of cell membranes by a dielectrophoresis method. Biophys J. 1991;59(5):982–7. 1831052. Available from: 10.1016/S0006-3495(91)82312-8.
32. Wipke BT, Allen PM. Essential role of neutrophils in the initiation and progression of a murine model of rheumatoid arthritis. J Immunol. 2001;167(3):1601–8. 11466382. Available from: 10.4049/jimmunol.167.3.1601.
33. Katsiari CG, Liossis SN, Sfikakis PP. The pathophysiologic role of monocytes and macrophages in systemic lupus erythematosus: a reappraisal. Semin Arthritis Rheum. 2010;39(6):491–503. 19147182. Available from: 10.1016/j.semarthrit.2008.11.002.
34. Fuss IJ, Kanof ME, Smith PD, Zola H. Isolation of whole mononuclear cells from peripheral blood and cord blood. In: Curr Protoc Immunol. USA: John Wiley & Sons, Inc; 2009. p. Chapter 7: Unit 7.1.
35. Bennett S, Breit SN. Variables in the isolation and culture of human monocytes that are of particular relevance to studies of HIV. J Leukoc Biol. 1994;56(3):236–40. 8083595. Available from: 10.1002/jlb.56.3.236.
36. Bennett S, Por SB, Stanley ER, Breit SN. Monocyte proliferation in a cytokine-free, serum-free system. J Immunol Methods. 1992;153(1-2):201–12. 1517590. Available from: 10.1016/0022-1759(92)90323-L.
37. Delirezh N, Shojaeefar E, Parvin P, Asadi B. Comparison the effects of two monocyte isolation methods, plastic adherence and magnetic activated cell sorting methods, on phagocytic activity of generated dendritic cells. Cell J. 2013;15(3):218–23. 24027662.
38. Hu P, Zhang W, Xin H, Deng G. Single Cell Isolation and Analysis. Front Cell Dev Biol. 2016;4:116. 27826548. Available from: 10.3389/fcell.2016.00116.
39. Tsuchiya S, Yamabe M, Yamaguchi Y, Kobayashi Y, Konno T, Tada K. Establishment and characterization of a human acute monocytic leukemia cell line (THP-1). Int J Cancer. 1980;26(2):171–6. 6970727. Available from: 10.1002/ijc.2910260208.
40. Schildberger A, Rossmanith E, Eichhorn T, Strassl K, Weber V. Monocytes, peripheral blood mononuclear cells, and THP-1 cells exhibit different cytokine expression patterns following stimulation with lipopolysaccharide. Mediators Inflamm. 2013;p. 697972. 23818743. Available from: 10.1155/2013/697972.
41. Bosshart H, Heinzelmann M. Lipopolysaccharide-mediated cell activation without rapid mobilization of cytosolic free calcium. Mol Immunol. 2004;41(10):1023–8. 15302164. Available from: 10.1016/j.molimm.2004.05.003.
42. Altieri DC, Edgington TS. The saturable high affinity association of factor X to ADP-stimulated monocytes defines a novel function of the Mac-1 receptor. J Biol Chem. 1988;263(15):7007–15. 2835359.
43. Kaplanski G, Marin V, Fabrigoule M, Boulay V, Benoliel AM, Bongrand P, et al. Thrombin-activated human endothelial cells support monocyte adhesion in vitro following expression of intercellular adhesion molecule-1 (ICAM-1; CD54) and vascular cell adhesion molecule-1 (VCAM-1; CD106). Blood. 1998;92(4):1259–67. 9694714.
44. Krakauer T. A sensitive ELISA for measuring the adhesion of leukocytic cells to human endothelial cells. J Immunol Methods. 1994;177(1-2):207–13. 7822828. Available from: 10.1016/0022-1759(94)90158-9.
45. Sneddon AA, McLeod E, Wahle KW, Arthur JR. Cytokine-induced monocyte adhesion to endothelial cells involves platelet-activating factor: suppression by conjugated linoleic acid. Biochim Biophys Acta. 2006;1761(7):793–801. 16829183. Available from: 10.1016/j.bbalip.2006.05.014.
46. Masuda S, Washizu M, Nanba T. Novel method of cell fusion in field constriction area in fluid integration circuit. IEEE Transactions on Industry. 1989;25(4):732–7. Available from: 10.1109/28.31255.
47. Cheng IF, Froude VE, Zhu Y, Chang HC, Chang HC. A continuous high-throughput bioparticle sorter based on 3D traveling-wave dielectrophoresis. Lab Chip. 2009;9(22):3193–201. 19865725. Available from: 10.1039/b910587e.

48. Broche LM, Labeed FH, Hughes MP. Extraction of dielectric properties of multiple populations from dielectrophoretic collection spectrum data. Phys Med Biol. 2005;50(10):2267–74. 15876666. Available from: 10.1088/0031-9155/50/10/006.
49. Huang Y, Wang XB, Becker FF, Gascoyne PR. Membrane changes associated with the temperature-sensitive P85gag-mos-dependent transformation of rat kidney cells as determined by dielectrophoresis and electrorotation. Biochim Biophys Acta. 1996;1282(1):76–84. 8679663. Available from: 10.1016/0005-2736(96)00047-8.
50. Mulhall HJ, Labeed FH, Kazmi B, Costea DE, Hughes MP, Lewis MP. Cancer, pre-cancer and normal oral cells distinguished by dielectrophoresis. Anal Bioanal Chem. 2011;401(8):2455–63. 21877186. Available from: 10.1007/s00216-011-5337-0.
51. Duncan L, Shelmerdine H, Hughes MP, Coley HM, Hübner Y, Labeed FH. Dielectrophoretic analysis of changes in cytoplasmic ion levels due to ion channel blocker action reveals underlying differences between drug-sensitive and multidrug-resistant leukaemic cells. Phys Med Biol. 2008;53(2):1–7. 18184986. Available from: 10.1088/0031-9155/53/2/N01.
52. Labeed FH, Lu J, Mulhall HJ, Marchenko SA, Hoettges KF, Estrada LC, et al. Biophysical characteristics reveal neural stem cell differentiation potential. PLoS One. 2011;6(9):e25458. 21980464. Available from: 10.1371/journal.pone.0025458.
53. Bisceglia E, Cubizolles M, Trainito CI, Berthier J, Pudda C, Francais O, et al. A generic and label free method based on dielectrophoresis for the continuous separation of microorganism from whole blood samples. Sens Actuators B Chem. 2015;212:335–43. Available from: 10.1016/j.snb.2015.02.024.
54. Wu L, Yung LYL, Lim KM. Dielectrophoretic capture voltage spectrum for measurement of dielectric properties and separation of cancer cells. Biomicrofluidics. 2012;6(1):14113–1411310. 22662097. Available from: 10.1063/1.3690470.
55. Hochmuth RM, Evans CA, Wiles HC, McCown JT. Mechanical measurement of red cell membrane thickness. Science. 1983;220(4592):101–2. 6828875. Available from: 10.1126/science.6828875.
56. Markx GH, Davey CL. The dielectric properties of biological cells at radiofrequencies. Application in biotechnology. Enzyme Microb Technol. 1999;25(3-5):161–71. Available from: 10.1016/S0141-0229(99)00008-3.
57. Irimajiri A, Hanai T, Inouye A. A dielectric theory of model with its application to a lymphoma cell. J Theor Biol. 1979;78(2):251–69. 573830. Available from: 10.1016/0022-5193(79)90268-6.
58. Jones TB. Electromechanics of Particles. Cambridge, New York, USA: Cambridge University Press; 2005.
59. Wang X, Wang XB, Gascoyne PR. General expression for dielectrophoretic force and electrorotational torque derived using the Maxwell stress tensor method. J Electrost. 1977;39(4):277–95. Available from: 10.1016/S0304-3886(97)00126-5.
60. Wang X, Becker FF, Gascoyne PR. The fractal dimension of cell membrane correlates with its capacitance: a new fractal single-shell model. Chaos. 2010;20(4):043133–1. 21198103. Available from: 10.1063/1.3526972.
61. Hu X, Arnold WM, Zimmermann U. Alterations in the electrical properties of T and B lymphocyte membranes induced by mitogenic stimulation. Activation monitored by electro-rotation of single cells. Biochim Biophys Acta. 1990;1021(2):191–200. 2302395. Available from: 10.1016/0005-2736(90)90033-K.
62. Gascoyne PR, Noshari BF, Pethig R. Use of dielectrophoretic collection spectra for characterizing differences between normal and cancerous cells. IEEE Trans Ind Appl. 1994;30(4):829–34. Available from: 10.1109/28.297896.
63. Dopp E, Jonas L, Nebe B, Budde A, Knippel E. Dielectric changes in membrane properties and cell interiors of human mesothelial cells in vitro after crocidolite asbestos exposure. Environ Health Perspect. 2000;108(2):153–8. 10656856. Available from: 10.1289/ehp.00108153.
64. Huang C, Liu C, Minne B, Hernandez JE, Stakenborg T, Lagae L. Dielectrophoretic discrimination of cancer cells on a microchip. Appl Phys Lett. 2014;105(14):143702. Available from: 10.1063/1.4897355.

Scan me